

Figure 1: Figure 1

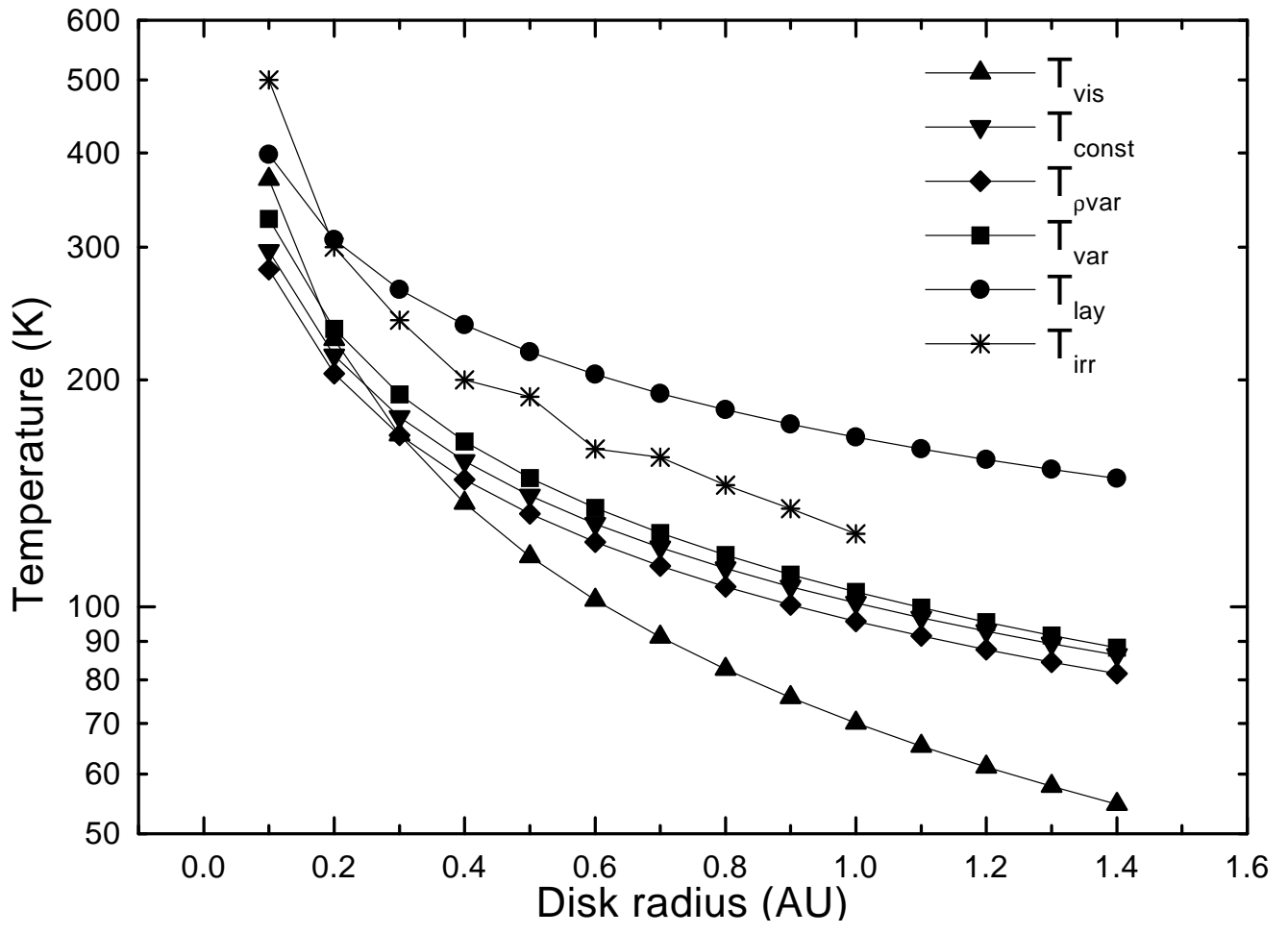


Figure 2: Figure 2a

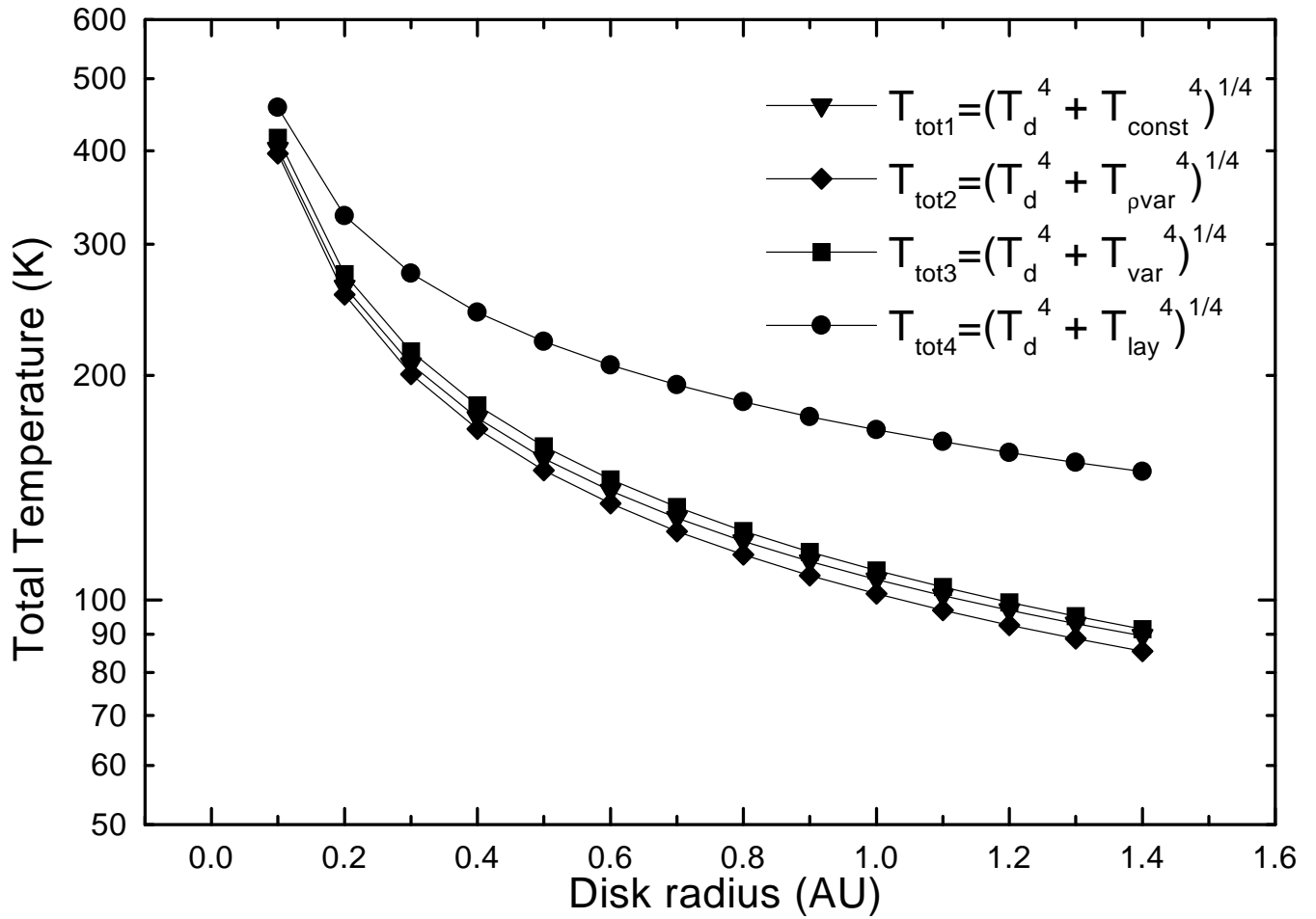


Figure 3: Figure 2b

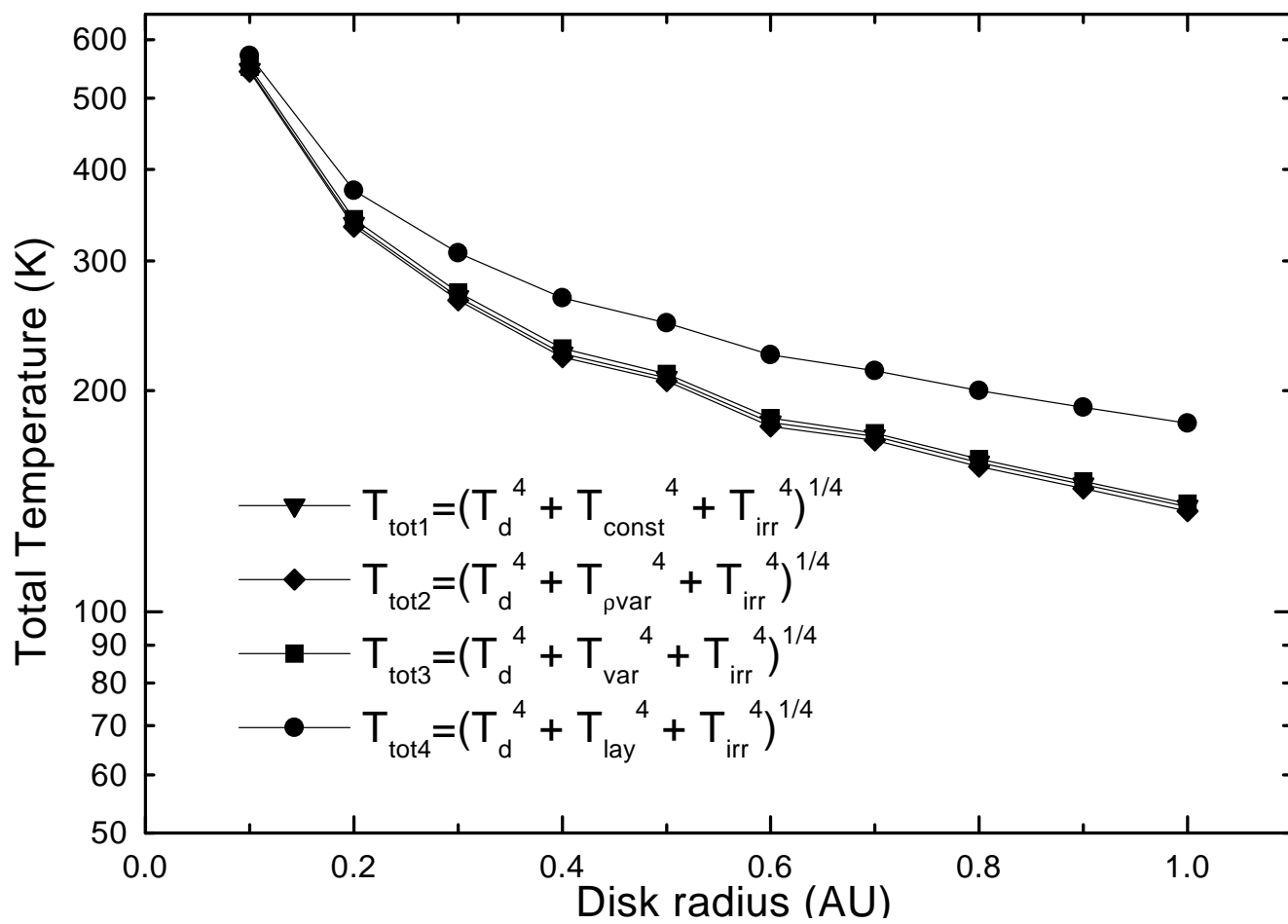


Figure 4: Figure 2c

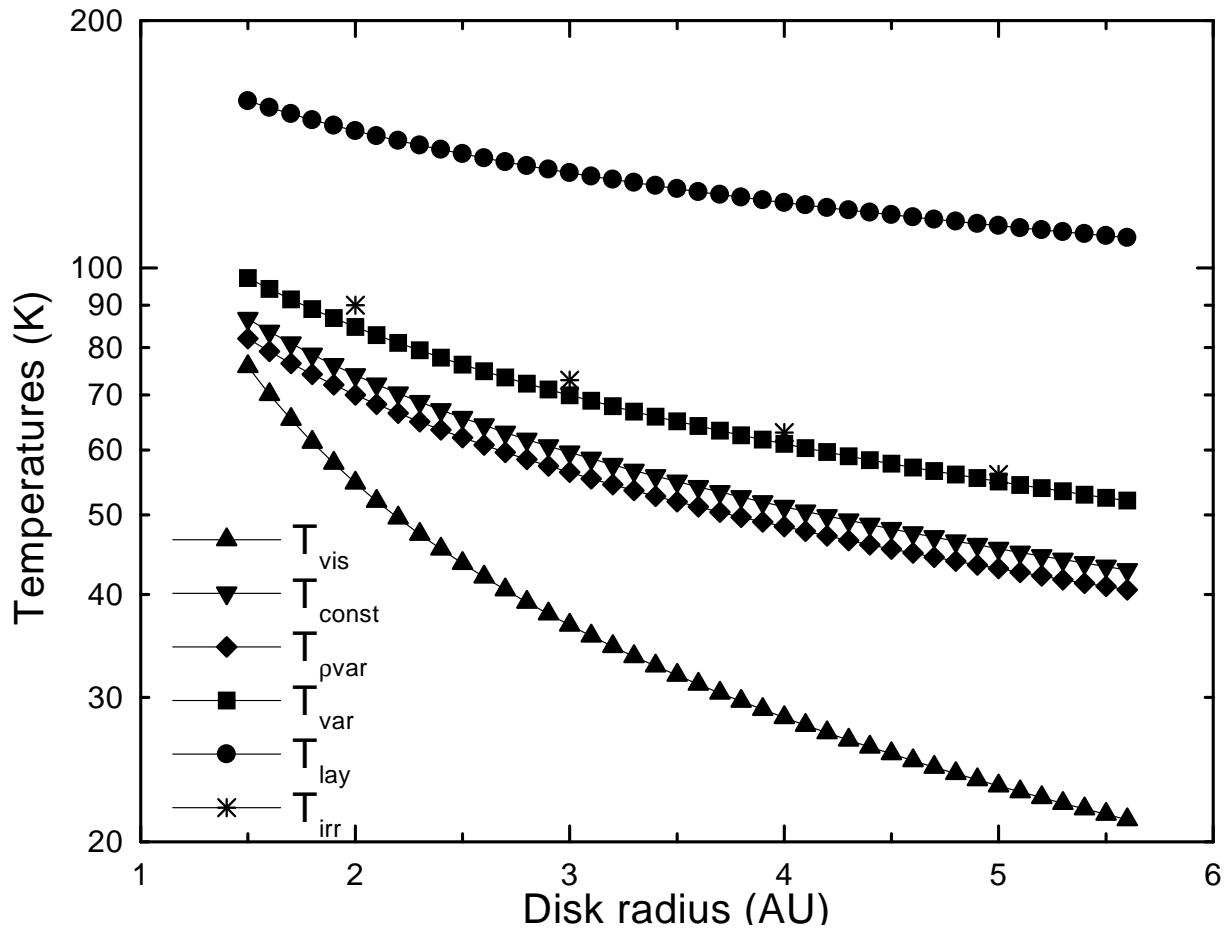


Figure 5: Figure 3a

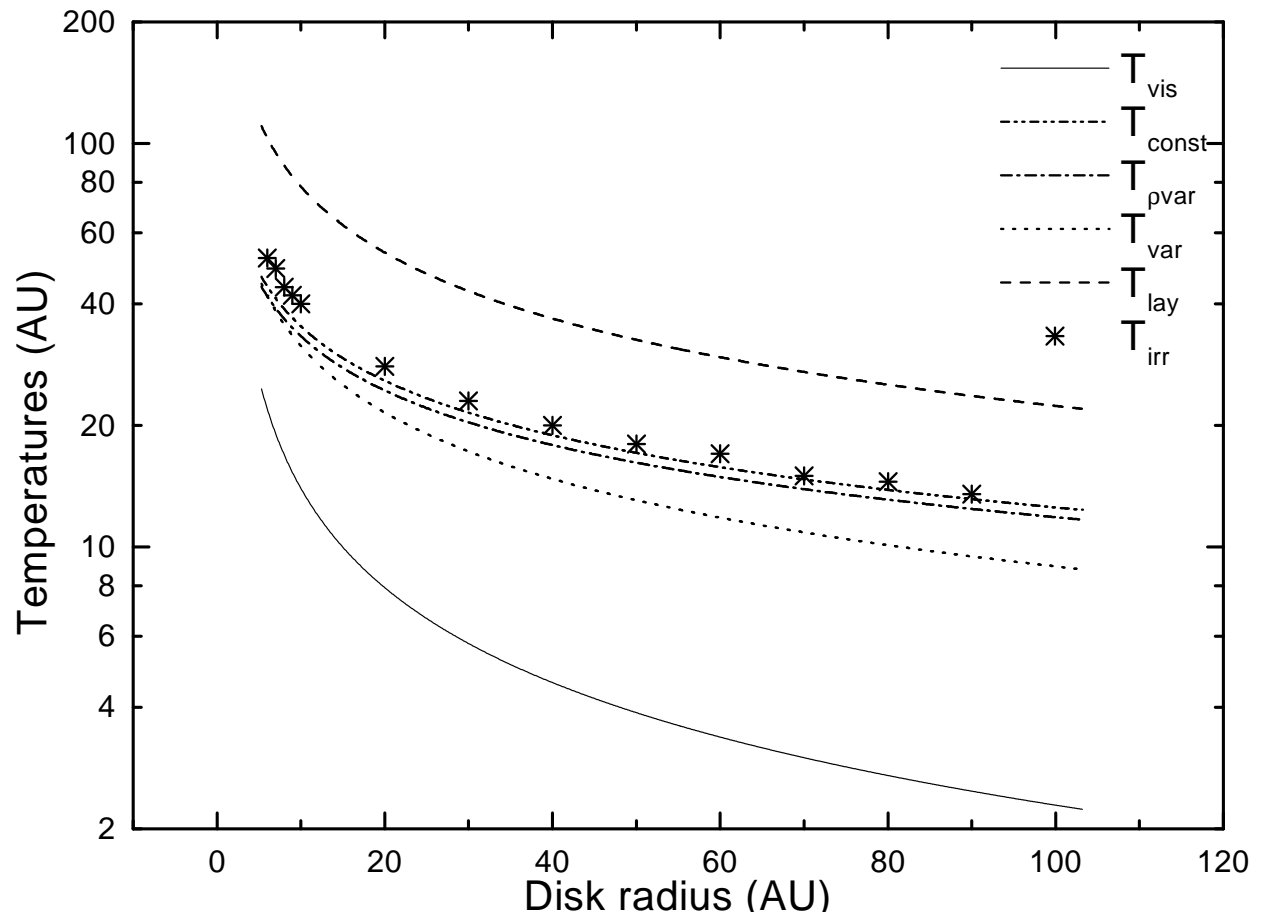


Figure 6: Figure 3b

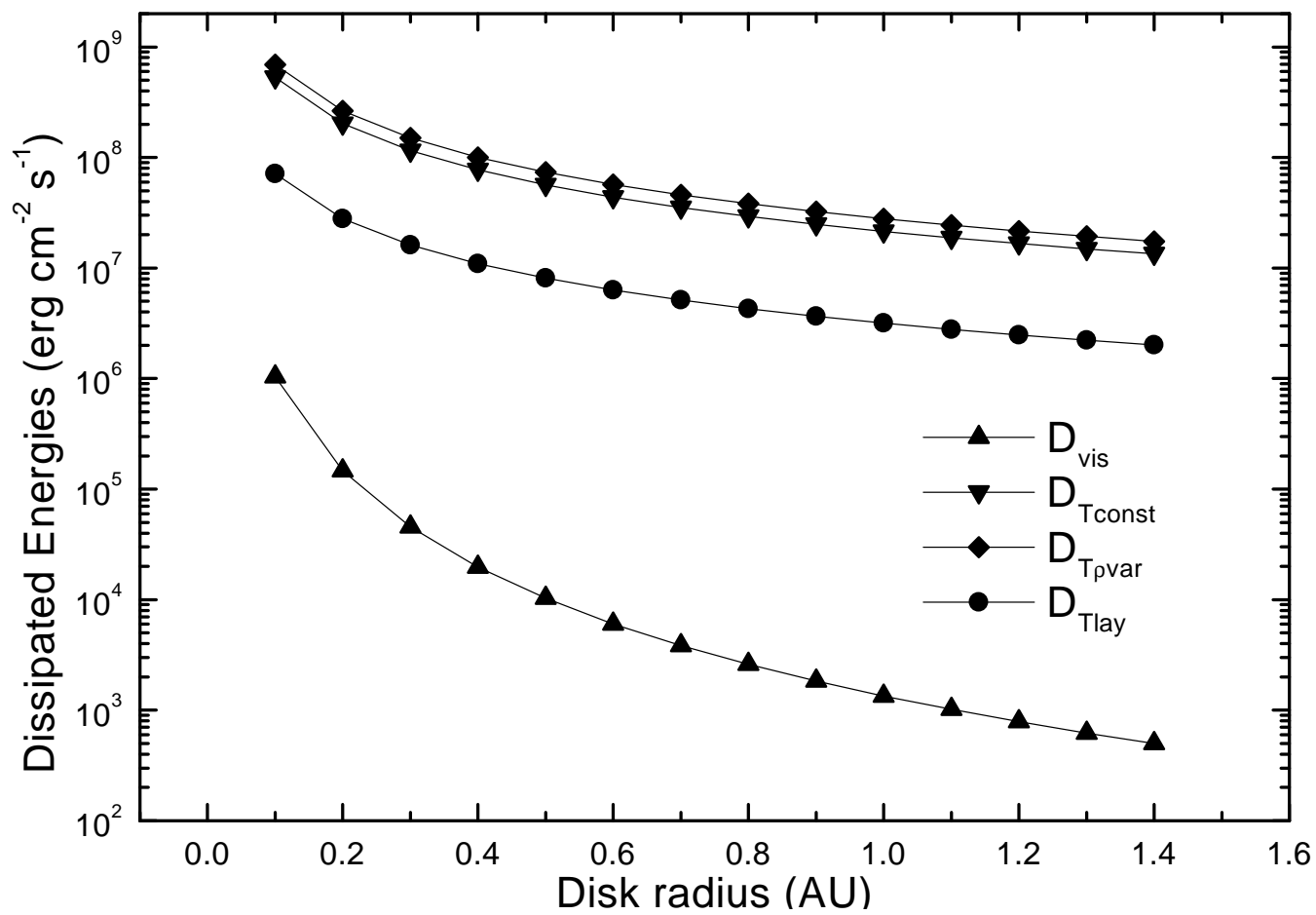


Figure 7: Figure 4a

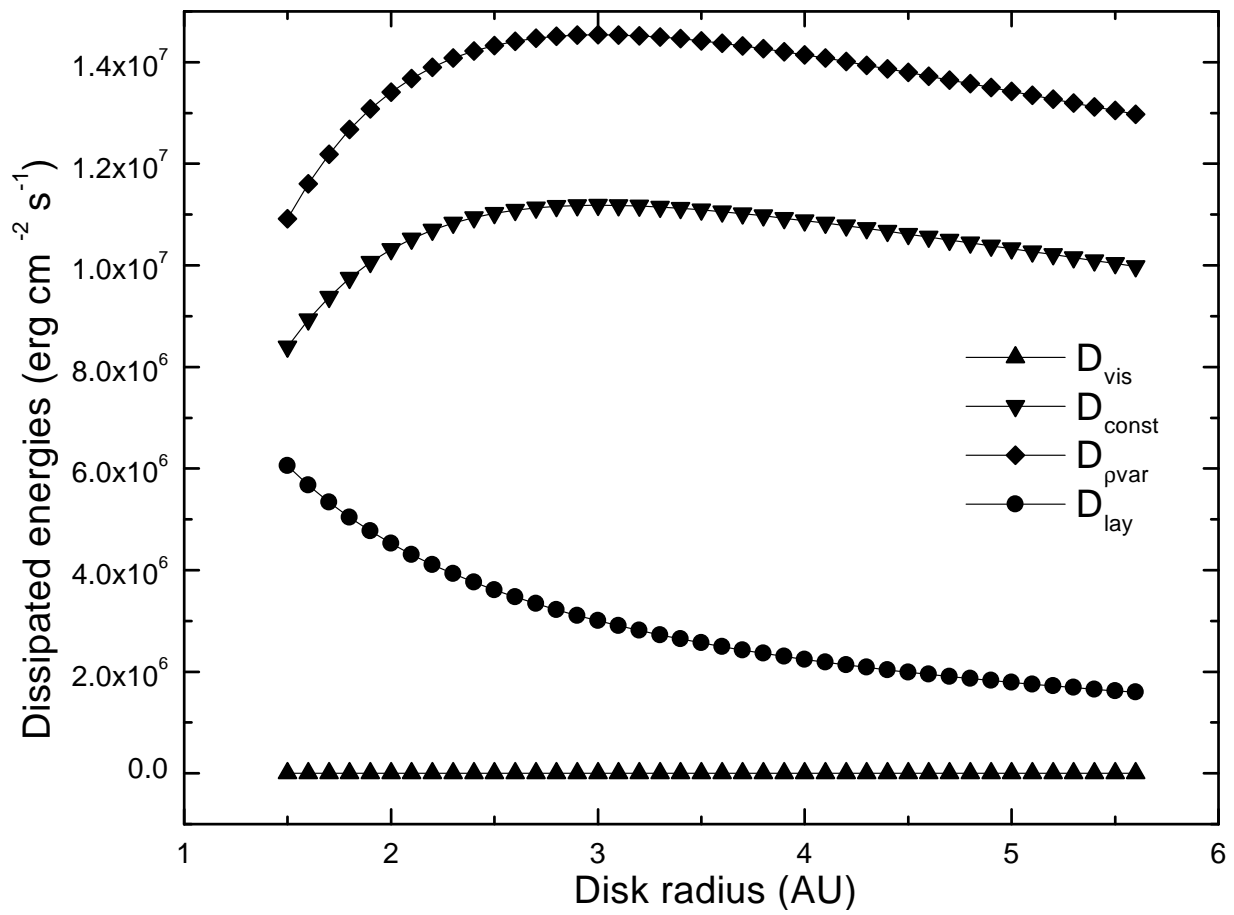


Figure 8: Figure 4b



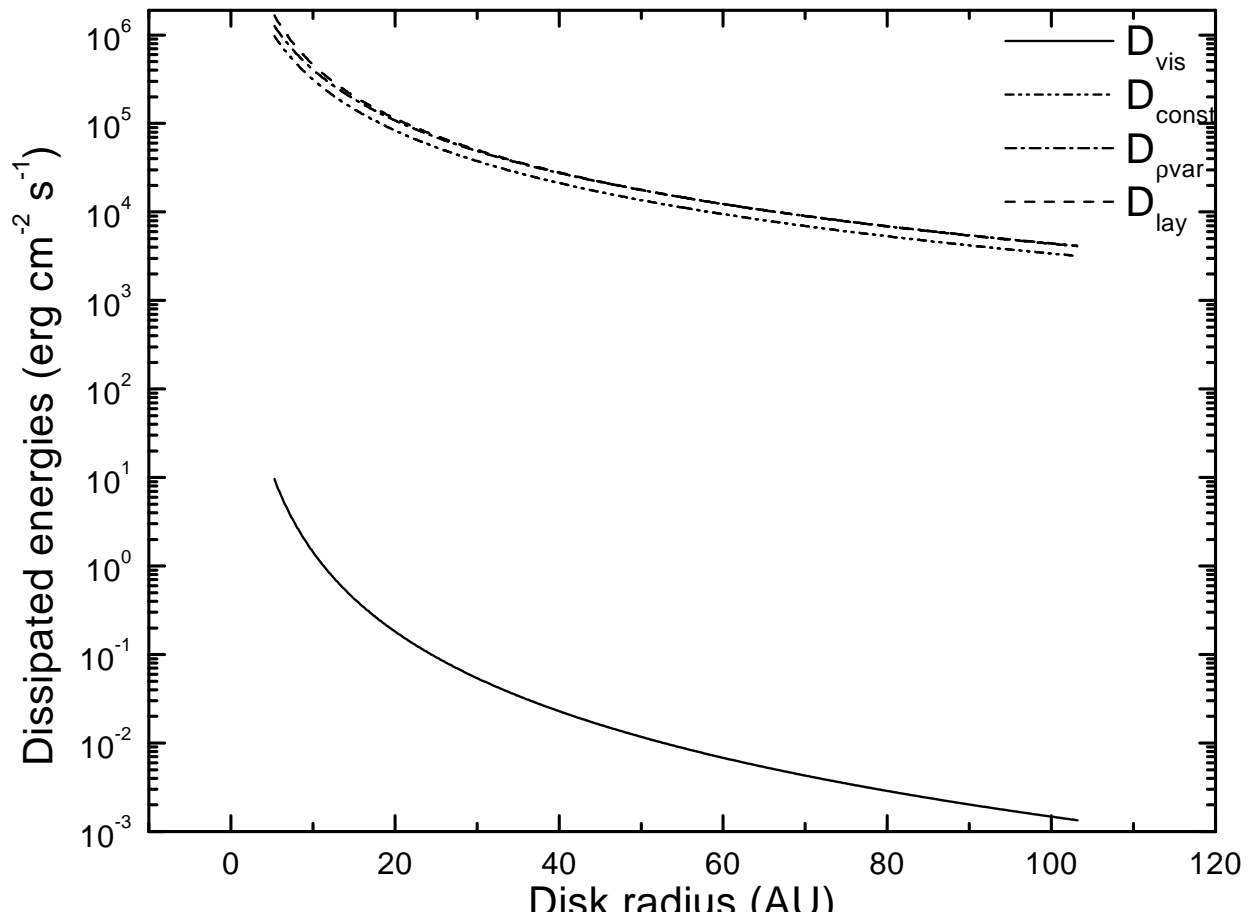


Figure 9: Figure 4c

# ALFVENIC HEATING OF PROTOSTELLAR ACCRETION DISKS

M. J. Vasconcelos, V. Jatenco-Pereira and R. Opher  
Instituto Astronômico e Geofísico, Universidade de São Paulo  
Av. Miguel Stéfano 4200, 04301-904 São Paulo, SP, BRAZIL  
jaque@iagusp.usp.br, jatenco@iagusp.usp.br, opher@iagusp.usp.br

## ABSTRACT

We investigate the effects of heating generated by damping of Alfvén waves on protostellar accretion disks. Two mechanisms of damping are investigated, nonlinear and turbulent, which were previously studied in stellar winds (Jatenco-Pereira & Opher 1989a, 1989b). For the nominal values studied,  $f = \delta v/v_A = 0.002$  and  $F = \varpi/\Omega_i = 0.1$ , where  $\delta v$ ,  $v_A$  and  $\varpi$  are the amplitude, velocity and average frequency of the Alfvén wave, respectively, and  $\Omega_i$  is the ion cyclotron frequency, we find that viscous heating is more important than Alfvén heating for small radii. When the radius is greater than 0.5 AU, Alfvénic heating is more important than viscous heating. Thus, even for the relatively small value of  $f = 0.002$ , Alfvénic heating can be an important source of energy for ionizing protostellar disks, enabling angular momentum transport to occur by the Balbus-Hawley instability.

*Subject headings:* accretion disks – MHD – stars: pre-main-sequence  
– waves

## 1. Introduction

Accretion disks are a powerful energy reservoir and are expected to be found around pre-main sequence objects and active galactic nuclei and in binary systems. One of the most challenging problems that still remains concerning these objects is the nature of the mechanism by which they transport angular momentum. A very promising mechanism was proposed some time ago by Balbus & Hawley (1991) (see also Balbus & Hawley 1998), based on a previously studied instability (Velikhov 1959, Chandrasekhar 1960). An ambient magnetic field, together with a differentially rotating system, can give rise to a powerful instability that is very effective in transporting angular momentum in the disk (e.g., Stone et al. 1996). However, because of its magnetic nature, the instability needs a minimum ionization density,  $(n_e/n_n) \gtrsim 10^{-13}$ , in order to be effective (Gammie 1996). The presence of this minimum ionization density in protostellar accretion disks is uncertain. Blaes & Balbus (1994) made a linear study of the Balbus-Hawley instability (BHI) in a partially ionized medium. Hawley & Stone (1998) did 3D numerical simulations and found that, in a disk that is not totally ionized, when  $0.01 < (\gamma\rho_i/\Omega) < 100$  (where  $\gamma\rho_i$  is the collision frequency and  $\Omega$ , the orbital frequency of the disk), there is angular momentum transport by BHI. Greater heating in the disk, in addition to that due to viscosity, will increase its degree of ionization and a larger fraction of the disk will be susceptible to the BHI. Our aim in this article is to analyze an extra source of plasma heating for the ionization of the neutral part of the disk, allowing the BHI to be effective in a greater part of it.

A system that is magnetized and turbulent implies the generation of MHD waves. These MHD modes can be damped by several mechanisms, including collisions between ionized and neutral particles, resistivity, electron viscosity, electron thermal conductivity, ion viscosity (Kulsrud & Pearce 1969) and mode coupling (Melrose 1980, Holzer et al. 1983, Zweibel & Josafatsson 1983). Damping of MHD modes can heat the gas. The damping of Alfvén waves has been considered to be a heating mechanism for the solar corona (e.g., Narain & Ulmschneider 1995) and in the heating of filaments in cooling flows in galaxy clusters (Friaç a et al. 1997). It has also been considered as a source of acceleration and heating of the solar wind (Jatenco-Pereira & Opher 1989a, Jatenco-Pereira et al. 1994), as well as a generating mechanism of winds in late-type giant stars (Holzer et al. 1983, Jatenco-Pereira & Opher 1989b).

There may be other sources of energy which can heat the disk, in addition to viscous heating. For example, D’Alessio et al. (1999) showed that the irradiation from the central star, as well as ionization by energetic particles may be important for heating the disk. The irradiation is most important for  $R \gtrsim 1$  AU. As discussed by the authors, stellar irradiation heats the dust, while the viscous dissipation heats the gas. If the gas and the dust are well

mixed, the disk will have the same temperature for both components. Alfvén waves will heat the gas, as will viscous dissipation. In principle, we can have these mechanisms (stellar irradiation, viscous dissipation and Alfvénic heating) all working together.

In general, the structure of a protostellar accretion disk is thought to be as shown schematically in Figure 1. Region 1 is the boundary layer between the disk and the star. This region can, in principle, extend up to the stellar surface. A difference in the rotational velocity of the two objects (disk and star) causes heating. The rotational velocity of the disk ( $\sim 260 \text{ km s}^{-1}$ ) is much greater than that of the star ( $\sim 10 \text{ km s}^{-1}$ ) and a large amount of energy is dissipated in a thin disk layer (Lynden-Bell & Pringle 1974). However, if the star has a strong magnetic field ( $\sim 1 \text{ kG}$ ; Wang 1996), it can disrupt the disk, with the accretion proceeding along the field lines (Ghosh & Lamb 1979a, b; Königl 1991). The magnetospheric accretion model accounts for many observational properties of T Tauri stars, such as the lack of a strong ultraviolet flux and the presence of blueshifted permitted lines (Edwards 1997). A controversial point in this class of models is the precise location of the place where the magnetic field truncates the disk (Hartmann 1998). Depending upon where this point (or region) is, the star can be spun up or down. Several wind models depend upon the determination of this location (e.g., Shu et al. 1994, 2000). Region 2 of the disk extends from  $\sim 0.01 \text{ AU}$  to  $\sim 1 \text{ AU}$  and is relatively close to the star. In this region, for  $0.01 \text{ AU} < R < 0.1 \text{ AU}$ , the temperature is above  $10^3 \text{ K}$ , which is sufficient to couple the magnetic field to the gas, and it is likely that the BHI is present here. However, when the temperature falls below  $10^3 \text{ K}$ , the role of BHI is uncertain. Region 3 in the figure extends from  $1.5 \text{ AU}$  to  $\sim 5 \text{ AU}$ . Gammie (1996) claims that for  $R \gtrsim 0.1 \text{ AU}$  the disk separates into three regions. Two regions, above and below the midplane of the disk are ionized by cosmic rays attaining the necessary temperature to couple the magnetic field with the gas. Cosmic rays, however, do not penetrate deep enough to heat the midplane region and the magnetic field is thought to decouple from the gas preventing the BHI from operating. Igea & Glassgold (1999) believe that X-rays from the central star are more effective in ionizing the disk than are cosmic rays. In region 4, the density of the disk is small enough for the disk to be totally ionized again. Somewhere in this region, the disk becomes optically thin and submillimeter observations provide information about the disk mass.

In this article, the extra source of heating for ionizing the neutral part of a protostellar accretion disk is assumed to be due to the damping of Alfvén waves. The damping mechanisms studied are nonlinear damping (section 2.1) and turbulent damping (section 2.2). For both damping mechanisms, we considered the cases of constant Alfvénic heating, exponentially varying density and temperature, as well as a layered model. We have made our calculations for the region that extends from  $0.1 \text{ AU}$  to  $\sim 100 \text{ AU}$ . The results and discussions are presented in section 3, our conclusions are given in section 4.

## 2. Alfvénic Heating

In order to quantify the amount of Alfvénic heating in a protostellar accretion disk we study the equations (in cylindrical coordinates) that describe a geometrically thin, optically thick, non-magnetized accretion disk (Pringle 1981, Hartmann 1998):

$$\frac{dF_z}{dz} = \frac{9}{4}\nu\rho\frac{GM_*}{R^3}, \quad (1)$$

$$\nu\Sigma = \frac{\dot{M}}{3\pi} \left[ 1 - \left( \frac{R_*}{R} \right)^{1/2} \right], \quad (2)$$

where  $F_z$  is the energy flux in the vertical  $z$  direction,  $\nu$  is the viscosity,  $\rho$  is the fluid density,  $G$  is the gravitational constant,  $M_*$  is the mass of the central star,  $R$  is the distance from the central star,  $\Sigma$  is the surface density and  $R_*$ , the radius of the central star.

Integrating equation (1), we obtain

$$F_z = \frac{9}{4}\nu\Sigma\frac{GM_*}{R^3}, \quad (3)$$

where we made use of the relation  $\Sigma = \int \rho dz$ . Substituting equation (2) into equation (3), we obtain the total flux of energy ( $\text{erg cm}^{-2} \text{s}^{-1}$ ) generated by viscous dissipation in the disk as a function of the disk radius:

$$F_z = D_{Tot} = D_{vis} = \frac{3GM_*\dot{M}}{8\pi} \left[ 1 - \left( \frac{R_*}{R} \right)^{1/2} \right] R^{-3}, \quad (4)$$

where  $\dot{M}$  is the accretion rate of the disk. Equation (4) is the gravitational potential energy liberated by the accretion flux. Since, in the present paper, we are examining the damping of Alfvén waves as an extra source of energy for heating the disk, we have

$$D_{Tot} = D_{vis} + D_A, \quad (5)$$

where  $D_A$  is the energy generated by the damping of Alfvén waves in the disk.

It is known that the nonlinear growth of the Balbus-Hawley instability results in turbulence (Stone et al. 1996) and so, we can have MHD modes traveling throughout the disk. These MHD modes can be damped by several mechanisms (e.g., Holzer et al. 1983, Zweibel & Josafatsson 1983). Here, we deal with two of these mechanisms: nonlinear damping and turbulent damping. These two damping mechanisms have been previously

investigated in a series of articles related to stellar winds by Jatenco-Pereira & Opher (1989a, 1989b) and Jatenco-Pereira et al. (1994). Here we investigate these damping mechanisms in relation to protostellar accretion disks.

High amplitude waves cause nonlinear mode couplings and, in this process, the resulting modes are rapidly damped. In general, the waves that result from the damping processes are sound waves; thus, the nonlinear Alfvénic energy is, in general, converted into thermal energy. If the Alfvén waves are not in phase, their energy is transferred both to the fast and slow magnetosonic modes (e.g., Holzer et al. 1983). In a high  $\beta$  plasma ( $\beta = 8\pi P/B^2 > 1$ , where  $P$  is the gas pressure and  $B^2/8\pi$ , the magnetic field pressure), the mode coupling of the Alfvénic mode to the slow magnetosonic mode can be very strong because the phase velocities of the modes are essentially the same (Melrose 1980).

Nonlinear damping of Alfvén waves requires waves of great amplitude  $\delta B/B$  (where  $\delta B$  is the amplitude of the magnetic field of the wave and  $B$  is the strength of the magnetic field of the medium). The turbulent damping mechanism requires the presence of turbulent cells or vortices. If we have a turbulent medium in which  $\delta B/B$  is large, in principle, we can have both mechanisms working together. In this paper we treat each mechanism separately.

In the next sub-section, we consider the nonlinear damping mechanism of Alfvén waves. (The damping rates used are obtained from Gonçalves et al. (1998), hereafter GJO).

## 2.1. Nonlinear damping of Alfvén waves

From equation (5), the total amount of heating in a magnetized accretion disk, assumed to be due only to Alfvén damping and viscosity, is

$$D_{Tot} = D_{vis} + \int_{-h}^{+h} H_A dz = D_{vis} + 2 \int_0^{+h} H_A dz, \quad (6)$$

where  $h$  is the half thickness of the disk,  $H_A = \Phi_w/L_A$  is the rate of Alfvénic heating,  $\Phi_w$  is the Alfvén wave flux,  $L_A = v_A/\Gamma_w$  is the damping length,  $v_A = B/\sqrt{4\pi\rho}$  is the Alfvén velocity and  $\Gamma_w$ , the damping rate of the waves. The nonlinear damping rate is given by

$$\Gamma_{NL} = \frac{1}{4} \sqrt{\frac{\pi}{2}} \xi \varpi \left( \frac{c_s}{v_A} \right) \frac{\rho \langle \delta v^2 \rangle}{B^2/8\pi}, \quad (7)$$

where  $\xi$  is a constant with a value between 5 and 10,  $\varpi$  is the characteristic frequency of the waves,  $c_s$  is the sound velocity and  $\rho \langle \delta v^2 \rangle / (B^2/8\pi)$ , the energy density of the waves divided by the magnetic energy density (GJO). The energy density of the waves can also

be written as (Whang 1997)

$$\epsilon_{Alfvén} = \frac{1}{2}\rho\langle\delta v^2\rangle + \frac{1}{8\pi}\langle\delta B^2\rangle. \quad (8)$$

The two terms on the right side of the equation (8) are generally equal, so that

$$\epsilon_{Alfvén} = \rho\langle\delta v^2\rangle. \quad (9)$$

Using the equations above, the wave flux can be expressed as

$$\Phi_w = \rho\langle\delta v^2\rangle v_A, \quad (10)$$

where  $\langle\delta v^2\rangle$  is proportional to the degree of turbulence of the system.

From equations (7) and (10), we obtain the nonlinear Alfvénic heating rate:

$$H_{NL} = \frac{\rho\langle\delta v^2\rangle v_A}{v_A} \frac{1}{4} \sqrt{\frac{\pi}{2}} \xi \varpi \left(\frac{c_s}{v_A}\right) \frac{\rho\langle\delta v^2\rangle}{B^2/8\pi}. \quad (11)$$

The adiabatic sound velocity is  $c_s = \sqrt{\gamma P/\rho}$  and, for an ideal gas,  $P = \rho\Re T/\mu$ , where  $\Re$  is the universal gas constant. We define the parameter  $f$  by

$$\langle\delta v^2\rangle = f^2 v_A^2. \quad (12)$$

The average frequency  $\varpi$  can be written as

$$\varpi = F\Omega_i = F \frac{eB}{m_i c}, \quad (13)$$

where  $F(< 1)$  is a free parameter,  $\Omega_i$  is the ion-cyclotron frequency and  $e$ ,  $m_i$  and  $c$  are the electron charge, the ion mass and the velocity of light, respectively.

Substituting equations (12) and (13) in equation (11), we have

$$H_{NL} = \frac{\sqrt{2}}{8} f^4 F \frac{e\xi}{m_i c} \left(\frac{\gamma\Re}{\mu}\right)^{1/2} (\rho T)^{1/2} B^2. \quad (14)$$

We then have, from equations (6) and (14)

$$D_{NL} = 2 \int_0^h H_{NL} dz = \frac{\sqrt{2}}{4} f^4 F \frac{e\xi}{m_i c} \left( \frac{\gamma \mathfrak{R}}{\mu} \right)^{1/2} \int_0^h (\rho T)^{1/2} B^2 dz. \quad (15)$$

Gammie (1996) proposed a model in which a protostellar accretion disk has different layers with different ionization rates. Near the star ( $R \lesssim 0.1\text{AU}$ ), the temperature is greater than  $10^3$  K and, thus, collisional ionization is sufficient to couple the gas to the magnetic field. Beyond  $R = 0.1\text{AU}$ , the temperature drops and only small layers above and below the central plane of the disk (called “active layers”) are able to sustain the Balbus-Hawley instability by cosmic ray ionization. The central layer, called the “dead zone”, is neutral, with insufficient ionization to enable coupling. The active layers have a constant surface density, which depends on the cosmic-ray ionization rate, a poorly known quantity. Gammie (1996) adopted the interstellar value (Spitzer & Tomasko 1968) for this rate and obtained  $\Sigma_a = 10^2 \text{ g cm}^{-2}$ , for the surface density of the active layers. Thus, if we assume that beyond the radius of 0.1 AU the surface density of the active layers is constant, we obtain from equation (15)

$$D_{NL} = \frac{\sqrt{2}}{4} f^4 F \frac{e\xi}{m_i c} \left( \frac{\gamma \mathfrak{R}}{\mu} \right)^{1/2} \Sigma_a^{1/2} \int_0^h T^{1/2} B^2 z^{-1/2} dz, \quad (R > 0.1\text{AU}), \quad (16)$$

where the relation  $\Sigma = \rho z$  was used and it is assumed that the thickness of the central neutral region is very small compared to the thickness of the active layers (Gammie 1996).

In quantifying the Alfvénic heating of a protostellar accretion disk, we consider various cases. The magnetic field in all of these cases, is held constant in the vertical direction, as was done in various previous papers (e.g., Stone & Norman 1994; Armitage 1998; Wardle 1999). First, we assume that the density and the temperature are constant throughout the disk (section 2.1.1). Then, we vary the density but still assume an isothermal disk (section 2.1.2). In the next case, we vary the temperature as well as the density (section 2.1.3). Finally (section 2.1.4), we consider the layered model of Gammie (1996). In the following subsections, we assume an average effective value for  $f$  and  $F$  in the disk.

### 2.1.1. Constant Nonlinear Alfvénic Heating

Considering the density, temperature and magnetic field to be constant throughout the disk, we integrate equation (15) and obtain



$$D_{NLconst} = \frac{\sqrt{2}}{4} f^4 F \frac{e\xi}{m_i c} \left( \frac{\mathfrak{R}}{\mu} \right)^{1/2} T_d^{1/2} B^2 \Sigma^{1/2} h^{1/2}, \quad (17)$$

where we used  $\gamma = 1$ , since the temperature is constant everywhere. The temperature  $T_d$ , adopted above, is obtained by assuming that the disk radiates as a blackbody and that the only source of dissipation is viscous heating. From  $D_{vis} = \sigma T_d^4$  (where  $\sigma$  is the Stefan-Boltzmann constant), we obtain

$$T_d^4 = \frac{3GM_* \dot{M}}{8\pi\sigma} \left[ 1 - \left( \frac{R_*}{R} \right)^{1/2} \right] R^{-3}. \quad (18)$$

### 2.1.2. Nonlinear Alfvénic Heating with Exponentially Varying density

According to the model of a stationary, geometrically thin accretion disk (Pringle 1981), if the temperature in the vertical direction is held constant, the resultant density profile is proportional to  $\exp(-z^2)$ . However, in a turbulent disk, it is expected that the decrease in density in the vertical direction is less dramatic, so that we assumed that the density falls as  $\exp(-z)$ . Thus, considering a disk with an exponentially varying density,  $\rho = \rho_c e^{-z/h}$ , equation (15) is given by

$$D_{NL\rho var} \simeq \frac{\sqrt{2}}{5} f^4 F \frac{e\xi}{m_i c} \left( \frac{\gamma \mathfrak{R}}{\mu} \right)^{1/2} (\rho_c T_d)^{1/2} B^2 h, \quad (19)$$

where we again used  $\gamma = 1$ .

### 2.1.3. Nonlinear Alfvénic Heating with Exponentially Varying density and Temperature

In order to obtain a consistent temperature profile in the vertical direction, it is necessary to solve the equations that describe the disk in the  $z$  direction (e.g., D’Alessio 1996; D’Alessio et al. 1998, 1999). This calculation requires a detailed treatment of the transport of the radiation and the advection of material by the BHI, which is beyond the scope of this paper. For simplicity, we have assumed that the temperature of the disk in the vertical direction falls off exponentially. So, in the case of a disk with both a density and temperature variation ( $T = T_c e^{-z/h}$ ) the Alfvénic heating is given by

$$D_{NLvar} \simeq \frac{3\sqrt{2}}{20} f^4 F \frac{e\xi}{m_i c} \left( \frac{\gamma \mathfrak{R}}{\mu} \right)^{1/2} (\rho_c T_c)^{1/2} B^2 h. \quad (20)$$

#### 2.1.4. The Layered Model

In this case, to quantify the amount of Alfvénic heating of the disk, we adopt the model of Gammie (1996). We consider only the region beyond 0.1 AU, where it is generally assumed that the disk is divided into three regions with different ionization densities. Adopting  $T = T_c$ , together with a constant magnetic field, and integrating equation (16), we obtain

$$D_{NLlay} = \frac{\sqrt{2}}{2} f^4 F \frac{e\xi}{m_i c} \left( \frac{\gamma \mathfrak{R}}{\mu} \right)^{1/2} (\Sigma_a T_c h)^{1/2} B^2 \quad (21)$$

## 2.2. Turbulent Damping

A damping length,  $L_T$ , can describe the absorption of turbulent Alfvén waves over a broad range of Alfvén periods. Similar to a Kolmogorov spectrum, a turbulent cascade transfers wave energy from large to small scale regions. The dissipation of energy through turbulence is governed by the small scale linear absorption mechanism. Noting the similarity of  $P_B \propto k^{-5/3}$  and Kolmogorov turbulence in ordinary fluids<sup>1</sup>, the volumetric heating rate associated with the cascade is  $H_T = \rho \langle \delta v^2 \rangle^{3/2} / L_{corr}$ , where  $L_{corr}$  is a measure of the transverse correlation length (Hollweg 1986). In terms of the damping length,

$$L_T = L_{corr} v \langle \delta v^2 \rangle^{-1/2}, \quad (22)$$

where  $L_{corr} \propto B^{-1/2}$  (Hollweg 1986) and  $v$  is the fluid velocity.

In the present work, we treat  $L_T$  as an independent damping process, although it may be connected with non-linear damping.

Then, the Alfvénic heating rate is given by (GJO)

---

<sup>1</sup>Where  $P_B$  is the observed magnetic power spectra in the solar wind and  $k$  is the wavenumber (Hollweg 1987).

$$H_T = \frac{\Phi_w B^{1/2} \langle \delta v^2 \rangle^{1/2}}{v_A} = \rho B^{1/2} \langle \delta v^2 \rangle^{3/2}. \quad (23)$$

Using equation (12), we obtain

$$H_T = \rho B^{1/2} f^3 v_A^3 = \left( \frac{f}{\sqrt{4\pi}} \right)^3 B^{7/2} \rho^{-1/2}. \quad (24)$$

In this case, the damping heating rate does not depend on temperature. Similar to our analysis in section 2.1, we consider three cases in order to obtain the total dissipation due to turbulent damping of Alfvén waves: 1) a disk with a constant density (section 2.2.1); 2) a disk with a variable density (section 2.2.2) and 3) a layered disk (section 2.2.3).

### 2.2.1. The Constant Turbulent Damping

We now consider a disk in which the density and the magnetic field are constant throughout. Integrating equation (24), we obtain

$$D_{Tconst} = 2 \left( \frac{f}{\sqrt{4\pi}} \right)^3 \left( \frac{B^7 h^3}{\Sigma} \right)^{1/2}. \quad (25)$$

### 2.2.2. Variable Density

Assuming that the density is varying exponentially with height ( $\rho = \rho_c e^{-z/h}$ ), we can integrate equation (24), obtaining

$$D_{Tvar} = 2.6 \left( \frac{f}{\sqrt{4\pi}} \right)^3 \left( \frac{B^7}{\rho_c} \right)^{1/2} h. \quad (26)$$

### 2.2.3. Layered Disk

Integrating equation (24), using the layered model of constant surface density ( $\rho = \Sigma_a/z$ ) (section 2.1.4), we obtain the total amount of heating for the turbulent damping of Alfvén waves,

$$D_{Tlay} = \frac{4}{3} \left( \frac{f}{\sqrt{4\pi}} \right)^3 \left( \frac{B^7 h^3}{\Sigma_a} \right)^{1/2}. \quad (27)$$

This equation is valid for the region beyond 0.1 AU, where it is assumed that there are active layers, created by cosmic ray ionization.

### 3. Results and Discussions

In Table 1, we show the values of the parameters of the disk that are used to calculate the different types of Alfvénic heating for region 2, except for those related to the layered model of Gammie (1996) ( $D_{NLlay}$  and  $D_{Tlay}$ ). These values (except the magnetic field) are obtained using a model of a stationary, geometrically thin, optically thick,  $\alpha$  accretion disk (e.g., Pringle 1981, Frank, King & Raine 1992, Shakura & Sunyaev 1973) with the opacity law of Bell & Lin (1994) in the iron-silicate regime<sup>2</sup>. The magnetic field is obtained from the model of Gammie (1996).

In Table 2, we show the disk parameters obtained from the model presented by Gammie (1996) for region 2. With the parameters shown in Table 2, we calculate the layered Alfvénic heating for region 2. The values of both models are obtained considering a disk surrounding a T Tauri star of  $0.5M_{\odot}$ , which is accreting mass at a rate of  $10^{-8} M_{\odot} \text{ year}^{-1}$ . We adopt a value of 0.6 for the mean molecular weight  $\mu$ .

Temperatures associated with each dissipated energy mechanism may be calculated, assuming that the disk radiates like a blackbody. Thus, there is the following temperature associated with  $D_{NLconst}$ , for example:

$$T_{const} = \left( \frac{D_{NLconst}}{\sigma} \right)^{1/4}, \quad (28)$$

where  $T_{const}$  is the temperature and  $\sigma$ , the Stefan-Boltzmann constant.

In Figure 2, we plot the temperatures associated with nonlinear Alfvénic dissipation for disk region 2, calculated from equation (28) with  $f = 0.002$  (eq. [12]),  $F = 0.1$  (eq. [13]) and  $\xi=5$ . Figure 2a shows the temperatures associated with each kind of dissipation.  $T_{vis}$  is obtained from the viscous dissipation of the stationary, geometrically thin accretion

---

<sup>2</sup>In this regime, the opacity is dominated by iron and silicate grains. The corresponding range of temperature is between  $\sim 10^3$  K to 203 K (Gammie 1996).

disk model (Table 1). For comparison, we plot  $T_{irr}$ , the temperature associated with the model of the irradiated disk (D’Alessio et al. 1998). Plotted values in the figure were obtained from Figure 3 of D’Alessio et al. (1998). The temperature calculated using Alfvénic dissipation in the layered model ( $T_{lay}$ , shown as circles in Fig. 2a) is highest for  $R \geq 0.2$  AU. The other temperatures ( $T_{const}$ ,  $T_{var}$ ,  $T_{\rho var}$ ) do not differ from one another very much.  $T_{vis} = (D_{vis}/\sigma)^{1/4}$  decreases with increasing radius, becoming less than the other temperatures for  $R > 0.4$  AU. The temperature obtained from the irradiated model is greater than  $T_{const}$ ,  $T_{\rho var}$ ,  $T_{var}$  for all radii considered. We plot the total temperatures obtained from our models together with  $T_{vis}$  in Figure 2b. They are calculated from the following relations:

$$T_{tot1} = [T_d^4 + T_{const}^4]^{1/4} = \left[ \frac{D_{vis}}{\sigma} + \frac{D_{NLconst}}{\sigma} \right]^{1/4}, \quad (29)$$

$$T_{tot2} = [T_d^4 + T_{\rho var}^4]^{1/4} = \left[ \frac{D_{vis}}{\sigma} + \frac{D_{NL\rho var}}{\sigma} \right]^{1/4}, \quad (30)$$

$$T_{tot3} = [T_d^4 + T_{var}^4]^{1/4} = \left[ \frac{D_{vis}}{\sigma} + \frac{D_{NLvar}}{\sigma} \right]^{1/4}, \quad (31)$$

$$T_{tot4} = [T_d^4 + T_{lay}^4]^{1/4} = \left[ \frac{D_{vis}}{\sigma} + \frac{D_{NLlay}}{\sigma} \right]^{1/4}. \quad (32)$$

We note the increase in temperature. Highest temperatures are again obtained when the layered model is used. The different density and temperature profiles, used to obtain the other Alfvénic dissipations ( $D_{NLconst}$ ,  $D_{NL\rho var}$  and  $D_{NLvar}$ ), do not affect the final total temperature obtained. They are practically equal for all radii.

In Figure 2c, we plot the total temperatures, taking into account the temperature from the irradiated model. The increase in temperature is much more significant than when only viscous dissipation is considered. Again, the density and temperature profiles do not alter the final temperature appreciably. The highest temperature is obtained from the layered model.  $T_{irr}$  dominates the total temperature values,  $T_{T1}$ ,  $T_{T2}$ ,  $T_{T3}$ , which indicates that irradiation may be more important than the Alfvénic heating mechanisms which produced  $T_{const}$ ,  $T_{\rho var}$ ,  $T_{var}$  for this part of the disk.

We further extend our calculations to include a larger amount of the protostellar disk. We divide the disk according to the different opacities laws, as given by Gammie (1996). We make our calculations for two additional regions (regions 3 and 4 of Figure 1). region 3 extending from 1.5 AU to 5.0 AU and region 4 extending from  $\sim 5$  AU to  $\sim 100$  AU. The opacity law for region 3 is given by  $\kappa = 2 \times 10^{16} T^{-7} \text{cm}^2 \text{g}^{-1}$  and for region 4, by  $\kappa = 2 \times 10^{-4} T^2 \text{cm}^2 \text{g}^{-1}$  (Bell & Lin 1994).

In Figure 3a, we show the temperatures obtained from nonlinear heating models, calculated for region 3 ( $1.5 \text{ AU} \leq R \leq 5 \text{ AU}$ ). For this region,  $T_{vis}$  (showed again as up triangles in figure) is the smallest temperature. The temperature obtained for the layered model (circles) is greater than that obtained for other models for all radii considered. The photospheric temperature obtained from the irradiated model is compared with  $T_{var}$  (stars and squares in the figure, respectively). In this figure, we note a small separation between the different profiles of temperature and density.

In Figure 3b, we plot the temperatures obtained from nonlinear heating models for region 4, which extends from  $\sim 5 \text{ AU}$  to  $\sim 100 \text{ AU}$ . We note small changes compared with Figure 3a. We can observe an inversion of the order of the temperatures. For this case,  $T_{var}$  is less than  $T_{const}$  and  $T_{\rho var}$ . However, this inversion is not very dramatic.  $T_{lay}$ , again, is the highest temperature and  $T_{irr}$  does not differ very much from the Alfvénic temperatures  $T_{const}$  and  $T_{\rho var}$ . In this part of the disk, the presence of layers with different degrees of ionization is less certain. Due to the small values of density, the penetration of cosmic rays can be deeper, perhaps, sufficiently to ionize this entire disk region.

In Figure 4a, we show the turbulent Alfvénic heating and viscous dissipation. For all radii, Alfvénic heating is greater than the viscous heating. This means that the turbulent mechanism for damping can be much more efficient to dissipate energy than the viscous mechanism. Moreover, we can see that, in this case, the turbulent Alfvénic heating calculated, using the layered model  $D_{Tlay}$  (eq. [27]), is less than both the Alfvénic heating with constant density  $D_{Tconst}$  (eq. [25]) and the Alfvénic heating with exponentially variable density  $D_{Tvar}$  (eq. [26]). However,  $D_{Tconst}$  and  $D_{Tvar}$  are practically the same for all radii. This means that turbulent damping is not very dependent on density. In Figure 4b, we plot the turbulent Alfvénic heating and viscous dissipation for region 3 ( $1.5 \text{ AU} < R < 5.0 \text{ AU}$ ). We note that viscous dissipation is very small, when compared with turbulent dissipation. For  $D_{\rho var}$  and  $D_{const}$ , there is a tendency for an increase at the beginning but after  $R \sim 3 \text{ AU}$  this tendency is reverted and the energy decreases. Again,  $D_{lay}$  is not very significant, when compared with the two other turbulent dissipations. In Figure 4c, we show the turbulent dissipated energies for region 4 ( $5 \text{ AU} \lesssim R \lesssim 100 \text{ AU}$ ). Again, turbulent dissipation is greater than viscous dissipation.

We know that an important parameter for disk models is the electron fraction,  $x = n_e/n_n$ , where  $n_e$  is the number density of electrons and  $n_n$ , the number density of the neutral specie. Gammie (1996) calculated an upper limit for this fraction, assuming ionization by cosmic rays. He obtained

$$x = \left( \frac{\zeta}{\beta n_H} \right)^{1/2} = 1.6 \times 10^{-12} \left( \frac{T}{500K} \right)^{1/4} \left( \frac{\zeta}{10^{-17} \text{s}^{-1}} \right)^{1/2} \left( \frac{n_H}{10^{13} \text{cm}^{-3}} \right)^{-1/2}, \quad (33)$$

where  $\zeta$  is the cosmic-ray ionization rate,  $\beta$  is the recombination coefficient and  $n_H$ , the number density of hydrogen. This expression is valid for  $T < 10^3$  K. Using equation (33) and  $T_d$ ,  $\Sigma$  and  $h$  from Table 2, we find that the electron fraction increases with radius. However, in order to evaluate  $x$ , Stone et al. (2000) used an expression derived from the Saha equation, which took into account the thermal ionization of potassium:

$$x = a^{1/2} T^{3/4} \left( \frac{2.4 \times 10^{15}}{n_n} \right)^{1/2} \exp(-50,370/2T), \quad (34)$$

where  $a$  is the abundance of potassium. In this case,  $x$  decreases with radius (The expression is valid for  $T < 2000K$ ). It is possible that, for the range of radii and temperature considered in this paper, the expression used by Gammie (1996) for  $x$  is the most likely to be valid. However, the determination of  $x$  is still very uncertain.

#### 4. Conclusion

In this paper, we analysed the important role that the damping of Alfvén waves may possibly play in the inner and intermediate regions of protostellar accretion disks ( $0.1 \leq R(\text{AU}) \lesssim 100$ ). We considered two damping mechanisms: nonlinear and turbulent.

We considered various profiles of density and temperature, with a constant magnetic field, in quantifying the heating generated by the damping of the waves. Concerning nonlinear damping, in the first case, the density and temperature are held constant throughout the disk. The resultant heating is called  $D_{NLconst}$ . In the second case, the density is exponentially varying, while the disk is isothermal ( $D_{NL\rho var}$ ). Both temperature and density are exponentially varying in the third case,  $D_{NLvar}$ . The heating  $D_{NLlay}$ , the fourth case, is obtained when nonlinear damping of Alfvén waves occurs in the disk model of Gammie (1996) (the layered model). We note that  $D_{NLlay}$  is greater than the viscous dissipation,  $D_{vis}$  for  $R \geq 0.2\text{AU}$ . We see that, for  $R > 0.5$  AU all the forms of nonlinear Alfvénic heating are greater than viscous heating. When the damping occurs by turbulent mechanisms, all the resultant turbulent Alfvénic dissipations are greater than viscous dissipation for all considered radii. Figure 2 shows the calculated temperatures for our model for region 1 ( $0.1 \text{ AU} \leq R \leq 1.4 \text{ AU}$ ). We note an increase in temperature for this region in Figure 2b. Thus, we conclude that, when viscous dissipation is insufficient to

ensure the necessary degree of ionization for BHI to occur, the damping of Alfvén waves can be an alternative source of energy for ionization. When taking into account the irradiation from the central star, the increase in temperature is much greater than when only the viscous dissipation is considered. Alfvénic heating in the layered model is very significant, greater than all other dissipations considered.

In Figures 3a and 3b we show the temperatures obtained from the nonlinear heatings for the outer parts of the disk. Again, the same order for the temperatures remains, with little differences shown. The viscous dissipation becomes smaller and less significant for increasing radii. The irradiation is a rather important source of heating, comparable with nonlinear Alfvénic  $D_{const}$ ,  $D_{\rho var}$  and  $D_{var}$ . In Figures 4b and 4c we see that turbulent dissipation is very efficient for heating the disk. We thus conclude that Alfvénic heating can be important in the outer parts of the disk. Considering only viscous dissipation, the temperatures reached are not sufficient to ensure the development of BHI and, consequently, of turbulence. If we take into account the irradiation from the central star, temperatures can reach values which ensure the necessary coupling between the gas and the magnetic field.

In the present paper, it is to be noted that we used  $f(\equiv \delta v/v_A) = 0.002$  and  $F(\equiv \varpi/\Omega_i) = 0.1$ . Nonlinear Alfvén heating is proportional to  $f^4 F$  and turbulent Alfvén heating, to  $f^3$ . Increasing (decreasing)  $f$  and  $F$  from these nominal values increases (decreases) the Alfvén heating. We have shown, in this paper, that even for the relatively small value of  $f = 0.002$ , Alfvénic heating can be important in protostellar disks.

M.J.V. would like to thank the Brazilian agency FAPESP for financial support. V.J.P and R.O. thank the Brazilian agency CNPq for partial support. The authors would like to also thank the project PRONEX/FINEP (No. 41.96.0908.00) for partial support.



## REFERENCES

- Armitage, P. J. 1998, *ApJ*, 501, L189
- Balbus, S. A., & Hawley, J. F. 1991, *ApJ*, 376, 214
- Balbus, S. A., & Hawley, J. F. 1998, *Rev. Mod. Phys.*, 70, 1
- Bell, K. R., & Lin, D. N. C. 1994, *ApJ*, 427, 987
- Blaes, O. M. & Balbus, S. A. 1994, *ApJ*, 421, 163
- Chandrasekhar, S. 1960, *Proc. Nat. Acad. Sci.*, 46, 53
- D'Alessio, P. 1996, PhD Thesis, Universidad Nacional Autonoma de Mexico
- D'Alessio, P., Cantó, J., Calvet, N. & Lizano, S. 1998, *ApJ*, 500, 411
- D'Alessio, P., Calvet, N., Hartmann, L., Lizano, S. & Cantó, J. 1999, *ApJ*, in press (astro-ph/9907330)
- Edwards, S. 1997, in *IAU Symp. 182, Herbig-Haro Flows and the birth of low-mass stars*, eds. B. Reipurth and C. Bertout, (Dordrecht: Kluwer), p.433
- Frank, J., King, A. R., & Raine, D. J. 1992, in *Accretion Power in Astrophysics*, 2nd. edition, (Cambridge: Cambridge University Press), p. 67
- Friaça, A. C. S., Gonçalves, D. R., Jafelice, L. C., Jatenco-Pereira, V., & Opher, R. 1997, *A&A*, 324, 449
- Gammie, C. F. 1996, *ApJ*, 457, 355
- Gonçalves, D. R., Jatenco-Pereira, V., & Opher, R. 1998, *ApJ*, 501, 797 (GJO)
- Ghosh, P., & Lamb, F. K. 1979a, *ApJ*, 232, 259
- Ghosh, P., & Lamb, F. K. 1979b, *ApJ*, 234, 296
- Hartmann, L. 1998, in *Accretion Processes in Star Formation*,(Cambridge: Cambridge University Press)
- Hawley, J. F. & Stone, J. M. 1998, *ApJ*, 501, 758
- Hollweg, J. V. 1986, *J. Geophys. Res.*, 91, 4111

- Hollweg, J. V. 1987, in Proc. 21st ESLAB Symposium on Small-Scale Plasma Processes, Norway
- Holzer, T. E., Flå, T., & Leer, E. 1983, ApJ, 275, 808
- Igea, J., & Glassgold, A. E. 1999, ApJ, 518, 848
- Jatenco-Pereira, V. & Opher, R. 1989a, ApJ, 344, 513
- Jatenco-Pereira, V. & Opher, R. 1989b, A&A, 209, 327
- Jatenco-Pereira, V., Opher, R. & Yamamoto, L. C. 1994, ApJ, 432, 409
- Königl, A. 1991, ApJ, 370, L39
- Kulsrud, R. & Pearce, W. P. 1969, ApJ, 156, 445
- Lynden-Bell, D., & Pringle, J. E. 1974, MNRAS, 271, 587
- Melrose, D. B. 1980, in Plasma Astrophysics: Nonthermal Processes in Diffuse Magnetized Plasmas, (New York: Gordon & Breach), vol.2, p.256
- Narain, U. & Ulmschneider, P. 1995, Space Science Reviews, 75, 453
- Pringle, J. E. 1981, ARA&A, 19, 137
- Shakura, N. I., & Sunyaev, R. A.: 1973, A&A, 24, 337
- Shu, F. H., Najita, J. R., Ostriker, E., Wilkin, F., Ruden, S., & Lizano, S. 1994, ApJ, 429, 781
- Shu, F. H., Najita, J. R., Shang, H. & Li, Z. -Y. 2000, in Protostars & Planets IV, ed. V. Mannings, A. P. Boss & S. S. Russel (Tucson: University of Arizona Press), in press
- Spitzer, L., & Tomasko, M. G. 1968, ApJ, 152,971
- Stone, J. M.,& Norman, M. L. 1994, ApJ, 433, 746
- Stone, J. M., Hawley, J. F., Gammie, C. F., & Balbus, S. A. 1996, ApJ, 463, 656
- Stone, J. M., Gammie, C. F., Balbus, S. A., & Hawley, J. F. 2000, in Protostars and Planets IV, ed. V. Mannings, A. P. Boss & S. S. Russel (Tucson: University of Arizona Press), in press
- Velikhov, E. P. 1959, Sov. Phys. JETP, 36, 995

Wang, Y. -M. 1996, ApJ, 465, L111

Wardle, M. 1999, MNRAS, 307, 849

Whang, Y. C. 1997, ApJ, 485, 389

Zweibel, E. L., & Josafatsson, K. 1983, ApJ, 270, 511

Fig. 1.— Sketch of a protostellar accretion disk. Region 1 corresponds to the boundary between the disk and the star. Region 2 extends from  $\sim 0.01$  AU to  $\sim 1$  AU. Region 3 extends from  $\sim 1$  AU to  $\sim 5$  AU. Beyond this region, region 4, the disk becomes optically thin. We make our calculations for regions 2,3, and 4, extending from 0.1 AU to  $\sim 100$  AU. (See text for a more detailed discussion.)

Fig. 2.— Temperatures associated with nonlinear Alfvénic dissipation, calculated for  $0.1 \text{ AU} < R < 1.4 \text{ AU}$ , assuming that the disk radiates like a blackbody. 2a) Each curve in this figure describes the temperature dependence vs radius calculated using the dissipation energy mechanism indicates (eq. [28]). The values attributed to  $T_{irr}$ , the temperature for an irradiated disk model was extracted from Figure 3 of D’Alessio et al. (1998); 2b) In this figure, we show the total temperatures reached in our models, taking into account only the viscous dissipation. They are obtained by summing the energy radiated by corresponding to viscous dissipation with the Alfvénic heatings (equations 29-32). 2c) This figure shows the total temperatures summing viscous dissipation, the irradiated model and each Alfvénic heating.

Fig. 3.— Temperatures associated with nonlinear Alfvénic dissipation, calculated for: 3a) for region 3 ( $1.5 \text{ AU} \leq R \leq 5 \text{ AU}$ ) and 3b) for region 4 ( $5 \text{ AU} \leq R \sim 100 \text{ AU}$ ).

Fig. 4.— Dissipated energies (in units of  $\text{erg cm}^{-2} \text{ s}^{-1}$ ) as a function of disk radius (in AU), obtained from the turbulent heating model, for: 4a) region 2 ( $0.1 \leq R \leq 1.4 \text{ AU}$ ), 4b) region 3 ( $1.5 \text{ AU} \leq R \leq 5 \text{ AU}$ ) and 4c) region 4 ( $5 \text{ AU} \leq R \sim 100 \text{ AU}$ ). We observe that turbulent Alfvénic heating is much greater than viscous heating for all density profiles.

Table 1. Parameters of a stationary, geometrically thin, optically thick protostellar accretion disk, with the opacity law of Bell & Lin (1994) in the iron-silicate regime.

R (AU)	$T_c$ (K)	$T_d$ (K)	h (AU)	$\Sigma$ (g cm <sup>-2</sup> )	$\rho_c$ (g cm <sup>-3</sup> )
0.1	1362.36	369.28	0.008	66.92	$5.31 \times 10^{-10}$
0.2	718.80	226.31	0.017	50.61	$1.95 \times 10^{-10}$
0.3	489.80	169.04	0.026	42.47	$1.08 \times 10^{-10}$
0.4	371.99	137.20	0.035	37.36	$7.09 \times 10^{-9}$
0.5	300.09	116.60	0.044	33.77	$5.11 \times 10^{-9}$
0.6	251.60	102.05	0.053	31.06	$3.90 \times 10^{-9}$
0.7	216.67	91.15	0.062	28.92	$3.11 \times 10^{-9}$
0.8	190.29	82.63	0.071	27.18	$2.55 \times 10^{-9}$
0.9	169.67	75.78	0.080	25.73	$2.14 \times 10^{-9}$
1.0	153.09	70.12	0.089	24.48	$1.83 \times 10^{-9}$
1.1	139.48	65.36	0.098	23.41	$1.59 \times 10^{-9}$
1.2	128.10	61.30	0.107	22.47	$1.40 \times 10^{-9}$
1.3	118.45	57.78	0.116	21.63	$1.24 \times 10^{-9}$
1.4	110.15	54.71	0.126	20.88	$1.11 \times 10^{-9}$

Note. — Here,  $R$  is the disk radius,  $T_c$  is the temperature of the midplane of the disk,  $T_d$  is the temperature due to viscous dissipation,  $h$  is the disk semi-thickness,  $B$  is the magnetic field (obtained from the model of Gammie 1996) and  $\rho_c$ , the midplane density.

Table 2. Parameters of the disk calculated using the layered model of Gammie (1996), for a region extending from 0.1 AU to 1.4 AU.

R (AU)	$T_c$ (K)	$T_d$ (K)	$h$ (AU)	$B$ (G)	$\rho_c$ (g cm <sup>-3</sup> )
0.1	1005.06	302.64	0.003	4.96	$3.51 \times 10^{-9}$
0.2	663.09	210.32	0.008	2.66	$1.53 \times 10^{-9}$
0.3	519.90	169.99	0.012	1.84	$9.40 \times 10^{-10}$
0.4	437.48	146.16	0.017	1.42	$6.66 \times 10^{-10}$
0.5	382.66	130.01	0.023	1.16	$5.09 \times 10^{-10}$
0.6	343.01	118.14	0.028	0.99	$4.09 \times 10^{-10}$
0.7	312.70	108.95	0.034	0.86	$3.40 \times 10^{-10}$
0.8	288.63	101.58	0.040	0.76	$2.90 \times 10^{-10}$
0.9	268.93	95.49	0.046	0.69	$2.51 \times 10^{-10}$
1.0	252.46	90.35	0.052	0.62	$2.22 \times 10^{-10}$
1.1	238.43	85.94	0.059	0.57	$1.98 \times 10^{-10}$
1.2	226.30	82.10	0.065	0.53	$1.78 \times 10^{-10}$
1.3	215.69	78.72	0.072	0.49	$1.62 \times 10^{-10}$
1.4	206.31	75.72	0.078	0.46	$1.48 \times 10^{-10}$

Note. — In this table,  $R$  is the disk radius,  $T_c$  is the temperature of the midplane of the disk,  $T_d$  is the temperature due to viscosity dissipation,  $h$  is the semi-thickness of the disk,  $B$  is the magnetic field and  $\rho_c$ , the midplane density.